J. Fluid Mech. (1975), *vol.* 70, *part* 3, *pp.* 573–593
Printed in Great Britain

Measurements in adverse-pressure-gradient turbulent boundary layers with a step change in surface roughness

By W. H. SCHOFIELD
Australian Defence Scientific Service, Aeronautical Research Laboratories,
Department of Defence, Victoria, Australia

(Received 7 June 1974)

The response of turbulent boundary layers to sudden changes in surface roughness under adverse-pressure-gradient conditions has been studied experimentally. The roughness used was in the '*d*' type array of Perry, Schofield & Joubert (1969). Two cases of a rough-to-smooth change in surface roughness were considered in the same arbitrary adverse pressure gradient. The two cases differed in the distance of the surface discontinuity from the leading edge and gave two sets of flow conditions for the establishment and growth of the internal layer which develops downstream from a change in surface roughness. These conditions were in turn different from those in the zero-pressure-gradient experiments of Antonia & Luxton. The results suggest that the growth of the new internal layer depends solely on the new conditions at the wall and scales with the local roughness length of that wall. Mean velocity profiles in the region after the step change in roughness were accurately described by Coles' law of the wall–law of the wake combination, which contrasts with the zero-pressure-gradient results of Antonia & Luxton. The skin-friction coefficient after the step change in roughness did not overshoot the equilibrium distribution but made a slow adjustment downstream of the step. Comparisons of mean profiles indicate that similar defect profile shapes are produced in layers with arbitrary adverse pressure gradients at positions where the values of Clauser's equilibrium parameter β ($= \delta^* \tau_0^{-1} dp/dx$) are similar, provided that the pressure-gradient history and local values of the pressure gradient are also similar.

1. Introduction

Theoretical and experimental work on the effects of discontinuous changes in boundary conditions on the development of turbulent shear flow has a relatively long history. Some of this work has been stimulated by practical problems (especially in the field of micrometeorology) but probably its experimental attraction lies in the proposal, advanced by Clauser (1956), that the problem appears to offer the possibility of understanding the internal exchange mechanisms of sheared flow. Both conduit and boundary-layer flows have been studied with perturbations applied at the wall, to the free stream and in the inner and outer regions of the layer itself. A general review of these results is available in

Tani (1968). So far the work has had limited success in revealing mechanisms of turbulent exchange. Even in the more straightforward task of defining the response of shear flows to perturbations, disagreements between results are not uncommon (for instance, on the validity of the universal law of the wall immediately after a small perturbation).

Some recent work by Antonia & Luxton (1971*a*, 1972) presents the most detailed and comprehensive measurements of a perturbed shear flow that are available. The problem studied was the development of a turbulent boundary layer in zero-pressure-gradient flow on a wall containing a sudden or step change in roughness. They concluded that to study these flows was essentially to study the development of the new internal layer which grows downstream of a step change in roughness† as flow outside this internal layer was unaffected by the new surface condition except for a small streamline displacement. Their papers are mainly concerned therefore with a detailed analysis and description of the growth and flow structure of the internal layer. Both the rough-to-smooth and smooth-to-rough case were considered. However, as their experiments were limited to one example of each under zero-pressure-gradient conditions, flow variables which dictated the growth of the new internal layer could not be distinguished. From a consideration of their results they suggested that the following variables may be important: (i) the flow structure upstream of the step, (ii) the structure of the flow downstream of the step but outside the new internal layer, (iii) the magnitude of the roughness step and (iv) the nature of the roughness before the step.

The starting point of the present experiments was to determine which (if any) of these variables determined the growth of the new internal layer. This was done by observing the growth of the internal layer in flows with the same type of wall discontinuity but with different values for the above variables. The flow conditions were also selected to be significantly different from those of the experiments of Antonia & Luxton.

The experiments were restricted to boundary-layer flows over a rough-to-smooth step, a case that has been studied by Taylor (1962) in a weak favourable pressure gradient, as well as by Antonia & Luxton. To obtain flow structures (both before the step and outside the internal layer after the step) which differed significantly from those of previous studies, flows in a strong adverse pressure gradient were investigated.

The roughness before the step was in a '*d*' type array to give a roughness different in nature from the more usual '*k*' type or sand-grain roughness used by Antonia & Luxton and Taylor. Physically a '*d*' type rough wall is characterized by deep closely spaced grooves transverse to the flow (as illustrated in figure 1). Flow-visualization studies by Perry *et al.* (1969) and Schofield (1969) have shown that the flow within these grooves is largely self-contained, being separated from the outer flow by a shear layer across the top of the cavity. The outer flow therefore rides over the crests of the roughness elements relatively undisturbed with little eddy shedding from the rough wall into the main flow. Conversely, at a '*k*' type rough wall there is strong interaction between flow over the crests of

† 'Step change in roughness' will be abbreviated to 'step' throughout this paper.

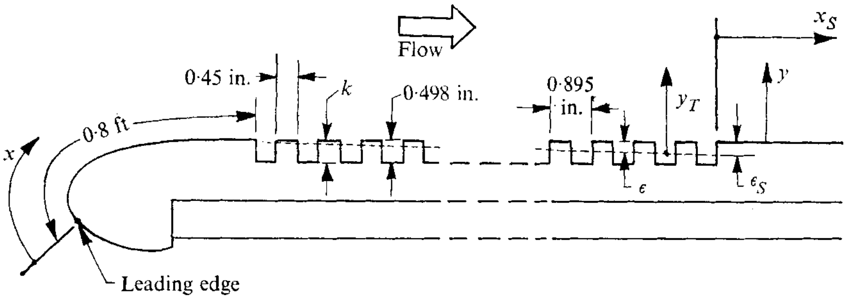

FIGURE 1. Diagram of test surface.

the elements and flow between the elements, resulting in strong eddy shedding into the main flow. Thus turbulence generated by the wall is significantly different for the two types of roughness (see Wood & Antonia 1974; Antonia & Luxton 1971*c*). This difference in surface flow behaviour is reflected in the functional dependence of the roughness function in Clauser's (1954) form of the logarithmic law of the wall, viz.

$$\frac{u}{u_\tau} = \frac{1}{\kappa}\log\frac{yu_\tau}{\nu} + A - \frac{\Delta u}{u_\tau}, \tag{1}$$

where κ and A are universal constants (taken here as 0·40 and 5·1), u the mean velocity, y the distance from the origin, $u_\tau = (\tau_0/\rho)^{\frac{1}{2}}$, τ_0 the wall shear, ρ the fluid density, ν the fluid kinematic viscosity and $\Delta u/u_\tau$ the roughness function.

For fully rough flow over a '*k*' type wall Clauser showed that

$$\frac{\Delta u}{u_\tau} = \frac{1}{\kappa}\log\frac{ku_\tau}{\nu} + D, \tag{2}$$

where k is a length representative of the roughness geometry (usually taken as the height) and D is a constant for a particular roughness. However (2) is not valid for '*d*' type roughness (Perry *et al.* 1969) as the dependent length scale in the roughness function is, for this case, the error in the origin of the mean velocity profile.† An important property of flow over a '*d*' type rough wall is that the error in the origin increases with development distance whereas it is a constant proportion of the roughness height for '*k*' type roughness.‡ This behaviour was used in the present experiment to vary the magnitude of the perturbation applied to the layer. By simply placing the leading edge of the smooth wall at different distances from the leading edge of the flow the magnitude of the perturbation

† The error ϵ in the origin of a mean velocity profile is the distance below the crests of the roughness elements that the effective origin of the mean profile must be located for the usual similarity laws to apply (see Moore 1951). The distance y in (1) must therefore be measured from this effective origin (y_T in figure 1).

‡ Thus (2) can be written more generally as

$$\frac{\Delta u}{u_\tau} = \frac{1}{\kappa}\log\frac{\epsilon u_\tau}{\nu} + E, \tag{3}$$

which applies to both '*k*' and '*d*' type roughness.

Layer	Roughness distribution	Length of rough wall	Nominal roughness height, k (in.)	Type of roughness	Error in origin at step, ϵ_S (in.)	$(\epsilon_S/\delta_S) \times 10^2$
R	Uniformly rough	x = 0·8–18·0 ft	0·5	'd'	—	—
S	Uniformly smooth	Nil	0	—	—	—
A	Rough to smooth	x = 0·8–11·5 ft	0·5	'd'	0·36	4·6
B	Rough to smooth	x = 8·0–9·6 ft	0·5	'd'	0·23	3·8
Antonia & Luxton (1971 a)	Smooth to rough	x = 8·0–16·0 ft	0·125	'k'	0	0
Antonia & Luxton (1972)	Rough to smooth	x = 8·0–12·0 ft	0·125	'k'	0·010†	3·5

† Value of ϵ_S not given in Antonia & Luxton (1972). This estimate was provided by Dr Antonia in a private communication.

TABLE 1. Wall roughness data. ϵ_S = error in origin at step, δ_S = total boundary-layer thickness at step, x = distance from the leading edge of the plate

at the step could be varied without varying the size of the roughness elements. Two positions of the step were investigated in the same adverse pressure gradient.

After a perturbation in zero-pressure-gradient flow the deviation from and return to equilibrium conditions can be readily assessed by reference to well-established properties of an undisturbed zero-pressure-gradient layer. For the present adverse-pressure-gradient flows it was necessary to have data from two reference flows: one over a uniformly smooth wall, the other over a uniformly rough wall but both in the same pressure gradient as was used in the perturbed flow tests.

2. Experiment

Previous publications (Perry 1966; Perry *et al.* 1969) have fully described the apparatus used in these experiments. The test boundary layers were formed on a flat plate 20 ft long and 4 ft wide which spanned the closed working section of a low turbulence, return-circuit wind tunnel. The plate was inclined at an angle of attack to the approaching flow such that a strong adverse pressure gradient was applied to its working face.

Details of the four roughness distributions used in these experiments are given in table 1. Exactly the same roughness geometry was used for series A and B (layers over a wall containing a rough-to-smooth step change in roughness) as for series R (a reference layer on a uniformly rough wall). Layer S was a reference layer on a uniformly smooth wall.† The roughness geometry was two-dimensional and fabricated by attaching rectangular slats of wood to the wall, transverse

† Layer-S results are Perry's, and have been previously reported in connexion with other work (Perry 1966).

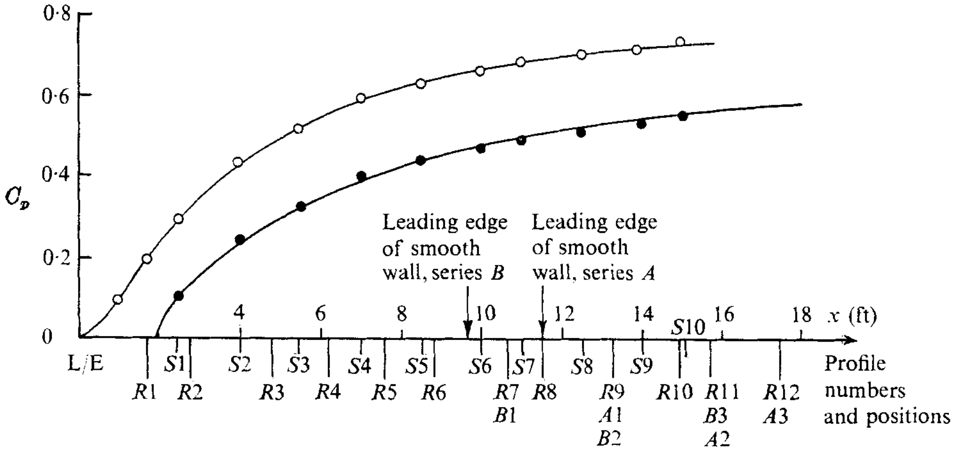

FIGURE 2. Pressure gradient and positions of measuring stations. —○—, smooth-wall reference layer (series *S*) as recorded by Perry (1966); ——, rough-wall reference layer (series *R*) and layers over a step (series *A* and *B*); ●, pressure gradient for series *S* adjusted for different reference-probe position.

to the flow. The slats were closely packed to give a roughness pattern with a pitch-to-height ratio of 1·8 which was the same as the '*d*' type pattern used by Perry *et al.* (1969). The crests of the roughness elements were aligned to have the same level as both the smooth leading edge of the plate and the smooth wall after the step in series *A* and *B* (see figure 1).

The pressure gradients for series *A*, *B* and *R* were identical while the pressure gradient for series *S* was closely comparable after allowance for a different reference-probe position had been made (see figure 2).

Mean velocity profiles were measured with a flattened Pitot tube† and separate static tube. Detailed profiles were measured for each of the four series at up to twelve stations spaced along the plate. All profiles measured on rough walls were in the 'fully rough' flow regime.

Skin-friction coefficients for the rough-wall flows‡ were determined by a method which analyses the momentum balance of a control volume around a single roughness element. This method requires detailed measurements of the pressure distributions on the vertical faces of a single roughness element and of the longitudinal pressure gradient in the layer. Details of the analysis and discussion of the assumptions involved in it are given in Perry *et al.* (1969) and Antonia & Luxton (1971*a*). The shear stress derived applies to a streamline some (small) distance above the crests of the elements but was used in the data reduction of Perry *et al.* as the true tangential shear of the layer. Their final results showed good internal consistency. However Reynolds-stress measurements by Antonia & Luxton (1971*a*) indicated that the shear stress derived by the method is accurate for a streamline not too close to the crests of the elements and hence may not be the true tangential stress. A direct comparison between the shear

† The opening of the probe had a wide rectangular form with dimensions $0·028 \times 0·15$ in.
‡ Skin-friction coefficients for series *S* were taken directly from Perry (1966).

stress given by the control-volume method and the wall shear given by well-established methods is described in Perry *et al.* For zero-pressure-gradient flow over a wall with uniform 'k' type roughness they found differences of the order of 10 % between stresses given by the control-volume method and the momentum-thickness distribution of the layer.

Perry *et al.* (1969) also illustrated a simple method for determining both the roughness function and the error in the origin of a rough-wall mean velocity profile, which requires a predetermined skin-friction coefficient and assumes the existence of a universal logarithmic distribution of mean velocity near the wall. It was applied to the present rough-wall profiles using the skin-friction coefficients determined by the control-volume method. Values thus obtained for the error in the origin of the layer showed the anticipated increase with development distance. The magnitudes of the error in the origin at the step for the two present series (A and B) were therefore significantly different both from each other and from that in the experiment of Antonia & Luxton (1972). Values of parameters are listed in table 1.

3. Results

Mean velocity profiles after a step are compared in figure 3 with corresponding profiles for the reference layer on a uniformly rough wall. The velocities are plotted against a stream function defined by

$$\psi = \int_0^y u\,dy.$$

Differences between the profiles of each pair appear to be small and in the outer regions of the profiles the agreement is almost within experimental accuracy. The correlation displayed by these profiles suggests that the longitudinal mean velocity in the outer regions of a layer over a step develops (at least initially) without knowledge of the new wall conditions. This has been noted in nearly all previous work on flows over wall perturbations (Tani 1968). However the response of the outer flow in this case appears to be slower than that in the rough-to-smooth, zero-pressure-gradient flow of Antonia & Luxton. At the station furthest from the step (station B 3†) differences between the perturbed and reference profiles are still very small. Antonia & Luxton's profiles at a comparable distance downstream show significant development towards a new self-preserving form.

Antonia & Luxton's results for a rough-to-smooth step gave streamlines that deflect towards the wall after the step, which is consistent with the analysis by Townsend (1965) of zero-pressure-gradient flow over a step. The streamline displacement is a consequence of velocity increases in the region of accelerated flow near the wall. The present flows differ considerably from the case analysed by Townsend. The whole flow is being decelerated by the adverse pressure gradient and at a very rapid rate in the region after the step, where the layer is approaching separation. The (small) acceleration due to the new wall conditions

† At a distance of twelve layer thicknesses downstream of the step.

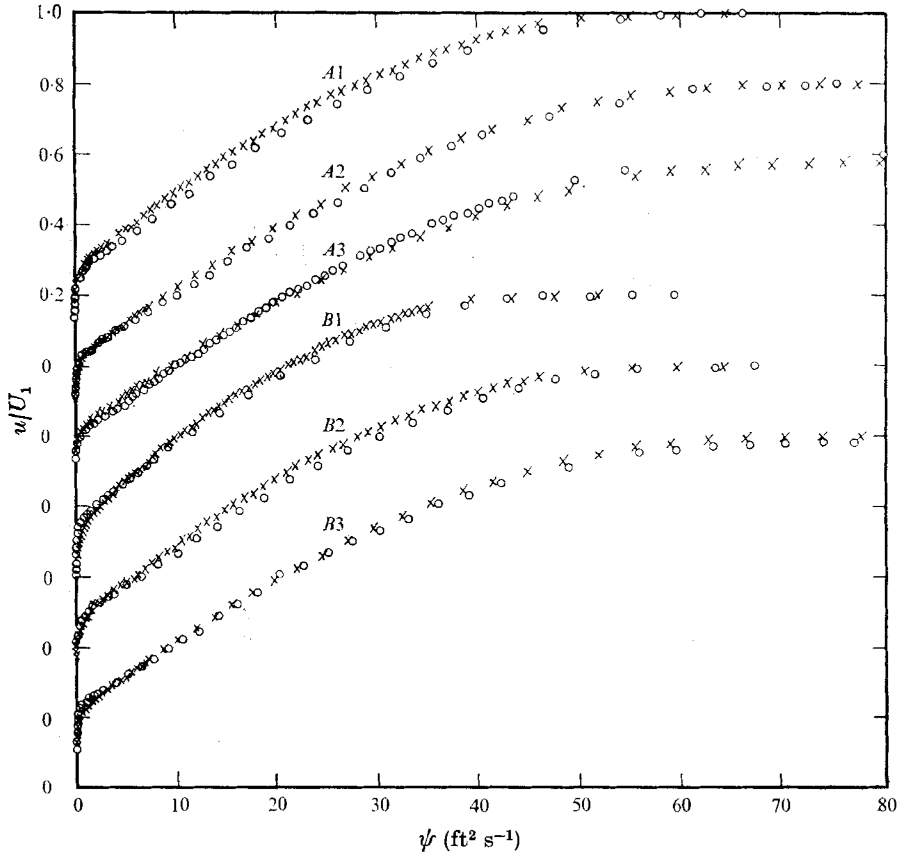

FIGURE 3. Smooth-wall mean velocity profiles after the step (circles) compared with rough-wall reference profiles (crosses) at the same situation. For clarity, experimental points near the wall have been omitted in all profiles.

after the step has a very minor effect on this gross behaviour and the streamlines continue to diverge rapidly from the wall. The positions of the streamlines for flow after a step were practically indistinguishable from those of the reference streamlines for flow over a uniformly rough wall.

3.1. *Internal layer*

The new wall conditions after the step abruptly change the wall shear stress and initiate a new flow structure, whose height grows within the boundary layer with increasing development distance. Antonia & Luxton inferred the height δ_i of this new internal layer by two methods. The physically more realistic method determined a position of 'merging' by superimposing mean velocity profiles obtained at closely spaced streamwise stations. In the present experiment the validity of this method was doubtful as the outer profile shape was changing rapidly in the adverse pressure gradient. In addition the profile stations were not closely spaced. For the present data 'merge' points were inferred by superimposing a profile after a step and the corresponding profile

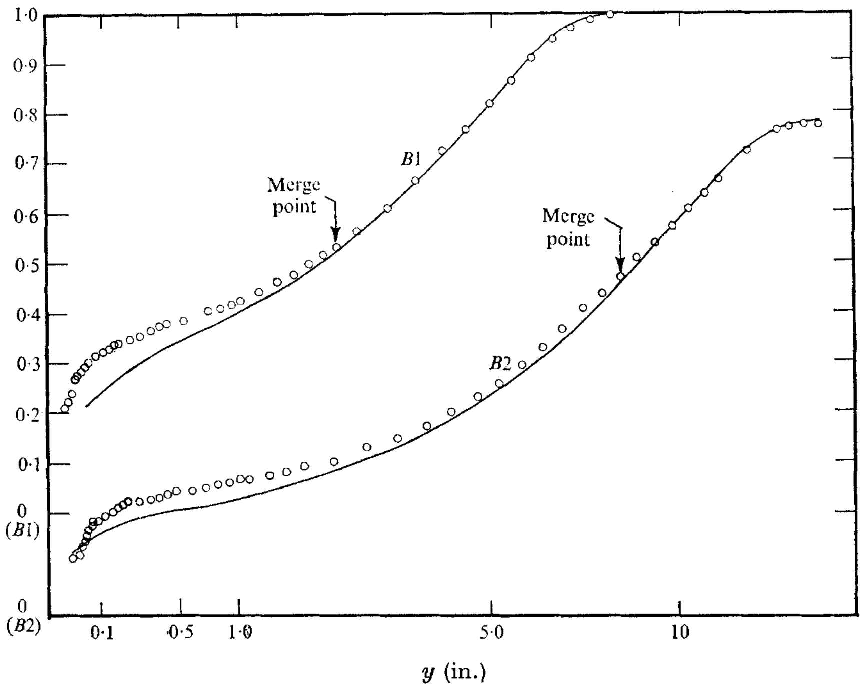

FIGURE 4. Examples of determination of 'merge' positions. ○, profile after step; ——, rough-wall reference profile. For clarity, experimental points near the wall have been omitted from both profiles.

from the rough-wall reference layer. Examples are shown in figure 4, where the Antonia & Luxton procedure of using a half-power scale for y has been retained to expand the profile in the region of interest. As the two profiles merge asymptotically the accuracy of δ_i is only fair in both these and Antonia & Luxton's data.

Antonia & Luxton fitted a simple power law to their data and obtained $\delta_i \propto x_S^{0\cdot43}$ for the rough-to-smooth step, which differed from their previous result $\delta_i \propto x_S^{0\cdot79}$ for a smooth-to-rough step. To compare data from different experimental conditions the appropriate non-dimensional form given by Townsend (1965) must be used. Townsend's analysis for zero-pressure-gradient flow over a step showed that the modified flow after a step scales with the (local) equivalent roughness length z, defined by expressing the logarithmic law of the wall [(1) and (2) or (3)] as

$$u/u_\tau = \kappa^{-1}\log(y/z). \tag{4}$$

Thus for flow over a 'k' type rough wall combination of (1), (2) and (4) gives for the equivalent roughness length

$$z = k\exp[\kappa(D-A)], \tag{5}$$

or more generally, using (1), (3) and (4),

$$z = \epsilon\exp[\kappa(E-A)], \tag{6}$$

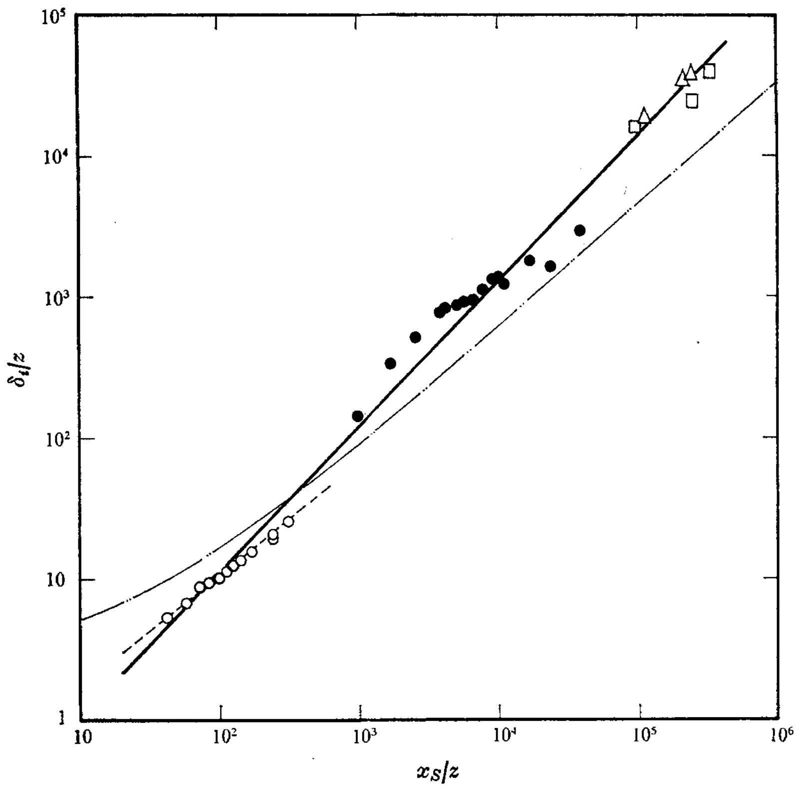

FIGURE 5. Growth of internal layer after a step change in roughness. △, series *A* (M = 5·0 to 5·3); □, series *B* (M = 4·8 to 5·3); ○, Antonia & Luxton (1971*a*), smooth-to-rough step (M = −4·6 to −5·1); ●, Antonia & Luxton (1972), rough-to-smooth step (M = 3·6 to 4·8); ——, equation (8); – – –, $\delta_i/z \propto (x_S/z)^{0\cdot 79}$; —··—, Townsend (1965).

which applies to both '*k*' and '*d*' type rough walls. The corresponding expression for smooth-wall flow is

$$z = \nu/[u_\tau \exp(\kappa A)]. \tag{7}$$

Figure 5 shows the growth rates of the internal layers in the Antonia & Luxton smooth-to-rough experiment, the present experiments and the Antonia & Luxton rough-to-smooth experiment, with δ_i and x_S non-dimensionalized using local equivalent roughness lengths determined from (5), (6) and (7) respectively.†

The values of z for the smooth wall for the rough-to-smooth data of Antonia & Luxton are based on values of skin friction inferred from the slope of the semi-logarithmic portions of the mean velocity profiles. Although the profiles did not

† There is of course an inconsistency here in that the validity of the universal logarithmic law is assumed whereas the Antonia & Luxton results show that such inner-layer similarity is probably not valid for their flows. However the above procedure was adopted by Antonia & Luxton (1971*a*) to determine z and the errors in such estimates of the wall length scale are unlikely to be large. It does mean that the accuracy of δ_i, which is based on fairly inaccurate estimates of the 'merge' point, is further degraded by expressing it as δ_i/z. This problem does not apply to the present data as they are shown to agree with the universal law of the wall in § 3.2.

agree with the universal logarithmic law of the wall these values of skin friction are preferable to the Preston-tube results as for the majority of the profiles the Preston tube used by Antonia & Luxton extended beyond the outer limit of the semi-logarithmic distribution.† For the rough-wall data the value of D [equation (2)] for the 'k' type wall was taken from Antonia & Luxton (1971*a*) and the value of E [equation (2)] for the 'd' type wall from Perry *et al.* The correlation of the three subsets of data with the line of best fit shown in figure 5 is reasonably good. This is particularly encouraging in view of the wide range of parameters over which the data extend. The roughness step parameter M, defined by Townsend as $M = \log(z_1/z_2)$ (z_1 = roughness length scale before the step, z_2 = roughness length scale after the step), varies within the data from $-5{\cdot}1$ to $+5{\cdot}3$. The line of best fit is given by

$$\log_{10}(\delta_i/z) = 1{\cdot}03\log_{10}(x_S/z) - 1{\cdot}02, \tag{8}$$

to which $\delta_i/z \propto x_S/z$ is an approximation within experimental accuracy. Townsend's expression for the growth of the internal layer, which written in a form similar to (8) is

$$\log_{10}(\delta_i/z) = \log_{10}(x_S/z) + \log_{10}\left[\frac{2\kappa^2}{\log(\delta_i/z) - 1}\right], \tag{9}$$

is also plotted in the figure. The validity of (9) is restricted in several important respects. The restrictions exclude flow at small x_S/z and in non-zero pressure gradients. Antonia & Luxton (1971*a*) have compared their smooth-to-rough results with (9) and explained the lack of agreement by the fact that Townsend's analysis requires inner-layer similarity throughout the flow while their results show this similarity to break down after the step. The agreement between Townsend's theoretical curve and data for the other experiments shown in figure 5 is also poor. However in all cases the flow did not conform to the case analysed. In both of Antonia & Luxton's flows inner similarity apparently did not apply after the step and the present experiment measured flow in a strong adverse pressure gradient. In spite of this, the overall trend of Townsend's prediction over five orders of magnitude in x_S/z is correct and the discrepancies not very much greater than the experimental scatter in the data points.

The line fitted by Antonia & Luxton to their data for smooth-to-rough flow is shown in figure 5 and is seen to fit the data rather better than (8). Similar lines could be fitted through each of the other two subsets of data which would correlate each group better than (8). If such lines were a correct description of the growth rates for each set of experimental conditions then factors of the type suggested by Antonia & Luxton would have to be taken into account in describing internal-layer growth in flow over a step. However, in the opinion of the present author the experimental conditions represented by the data in figure 5 are so different that the correlation with (8) is sufficiently good to support the view that the internal-layer growth is simply dependent on the nature of the new wall alone and scales with the local equivalent roughness length of that wall.

† I am indebted to Dr Antonia for supplying much original data from their experiments, some of which were not given explicitly in their papers.

3.2. *Inner-flow similarity and wall shear*

Antonia & Luxton concluded that the universal logarithmic law of the wall did not apply in zero-pressure-gradient flow after a step change in roughness. This conclusion was based first on turbulence measurements, which showed that the wall region was not in equilibrium in the sense described by Townsend (1961), and hence that there was little physical basis to support the existence of the universal law, and second, on the fact that, although mean velocity profiles displayed logarithmic distributions, they were not 'universal' as the constants implied by the distributions varied significantly from the accepted 'universal' values. This result differed from previous work. Universal logarithmic distributions of velocity after a step were reported in two previous experiments that were similar to the cases studied by Antonia & Luxton (Taylor 1962; Makita 1968†). Universal distributions were also found in flows subjected to other types of sudden perturbation (Bradshaw 1969, sudden application of pressure gradient; Bradshaw & Ferriss 1965, sudden removal of pressure gradient). Other perturbed flows in which universal wall similarity was not rapidly established were characterized by the generation of a significant separation region by the perturbation (Tillmann 1945‡; Bradshaw & Wong 1972; Antonia & Luxton 1971*b*). However, as the results of Antonia & Luxton are the most detailed and extensive available, their conclusion of the breakdown of wall similarity after a step must be regarded as probably correct for at least the zero-pressure-gradient case involving '*k*' type roughness.

The inner regions of the present profiles are plotted in semi-logarithmic coordinates in figure 6.§ They are compared with the universal law of the wall [equation (1)] expressed in Clauser's (1954) form:

$$\frac{u}{U_1} = 5{\cdot}76\,(c_f'/2)^{\frac{1}{2}}\log_{10}\frac{yU_1}{\nu} + 5{\cdot}76(c_f'/2)^{\frac{1}{2}}\log_{10}(c_f'/2)^{\frac{1}{2}} + 5{\cdot}1(c_f'/2)^{\frac{1}{2}},$$

where c_f' is the local skin-friction coefficient. The results show good agreement with the universal form for profiles as close as two layer thicknesses from the step (profile $B1$). The outer extent of the agreement varies between 0·1 and 0·12 of the total layer thickness. Similar heights were found in corresponding profiles of the undisturbed reference layers.

The validity of mean flow wall similarity in the present flows after the step is probably a consequence of the '*d*' type roughness before the step. As discussed previously the turbulence structure near a '*d*' type rough wall does not differ greatly from that near a smooth wall (Wood & Antonia 1974). Thus transition from a '*d*' type rough wall to a smooth wall requires only a minor adjustment in the turbulence structure and gives rapid establishment of wall similarity. This contrasts with flow over a '*k*' type rough wall, where the turbulence structure is quite different (Antonia & Luxton 1971*c*) from smooth-wall turbulence.

† Some results by Makita are quoted in Tani (1968). Makita studied a rough-to-smooth step in fully developed channel flow.

‡ See discussion in Coles (1968, p. 15).

§ The profiles have not been corrected for probe displacement or turbulence effects.

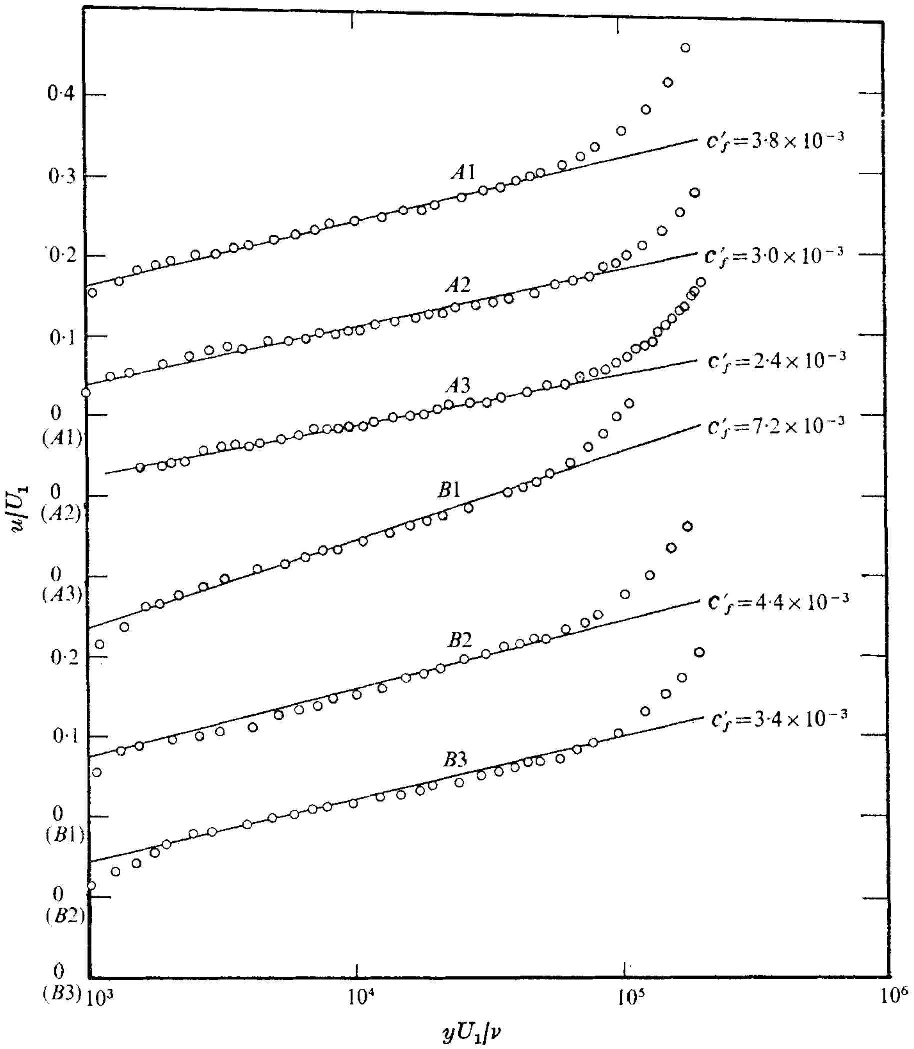

FIGURE 6. Inner-flow profiles after a step change in roughness. ——, equation (9).

Variations in the skin-friction coefficient for the two layers over a step are compared with those of the two reference layers in figure 7. It appears that the wall shear attains, but does not overshoot, the equilibrium distribution immediately after the step. This result contrasts with the behaviour in zero-pressure-gradient and ducted flows noted by Tani (1968) and Coles (1968) in their review articles. Both concluded that overshooting of the equilibrium value by the wall shear was a feature of sheared flows after a wall discontinuity although the degree of overshoot was small in the absence of complete separation and reattachment. The present data also show a slow divergence from the equilibrium distribution after a step, rather than the slow convergence demonstrated by Coles for the zero-pressure-gradient data of Klebanoff & Diehl (1951) and Tillmann (1945). The skin-friction coefficients of both perturbed layers show a

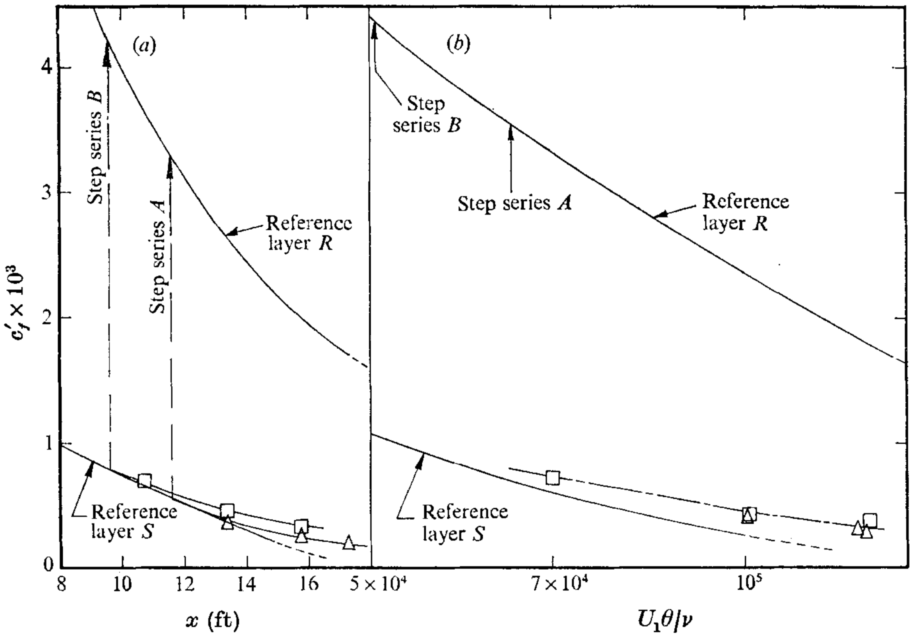

FIGURE 7. Distribution of skin-friction coefficient (*a*) as a function of distance and (*b*) as a function of momentum-thickness Reynolds number. △, series *A*; □, series *B*; — — —, Ludwieg & Tillmann skin-friction formula.

correlation with momentum-thickness Reynolds number which is well described by the standard Ludwieg & Tillmann skin-friction formula. As Bradshaw & Wong (1972) have noted, if the discontinuity does not destroy wall similarity then a major change in profile shape is required to invalidate the relationship between the wall shear stress and the integral thickness parameters, which is expressed in formulae of the Ludwieg & Tillmann type.

3.3. *Profile parameters and equilibrium criteria*

Figures 3 and 4 showed that the outer mean flow profiles of series *A* and *B* are very similar to corresponding profiles of series *R*. These similar outer profiles are matched in the two types of layers to inner layers in which the wall shear stress differs by almost an order of magnitude. Coles' (1956) wake hypothesis relates the outer flow to the wall shear by the expression

$$u = u_\tau f\left(\frac{yu_\tau}{\nu}\right) + u_\tau \frac{\Pi}{\kappa}\, \omega(y/\delta_c), \tag{10}$$

where f and ω are functions tabulated by Coles (1953, 1956), Π is the wake strength factor and δ_c the Coles' total-layer thickness. The present data were seen as presenting a demanding test of this hypothesis as the same outer flow had to be correlated with two divergent values of the velocity scale u_τ with only one adjustable constant (Π). Coles (1968) recognized that flow over a wall discontinuity is a case in which (10) often gives inaccurate profile descriptions. However the data from which he drew this conclusion were restricted, and had

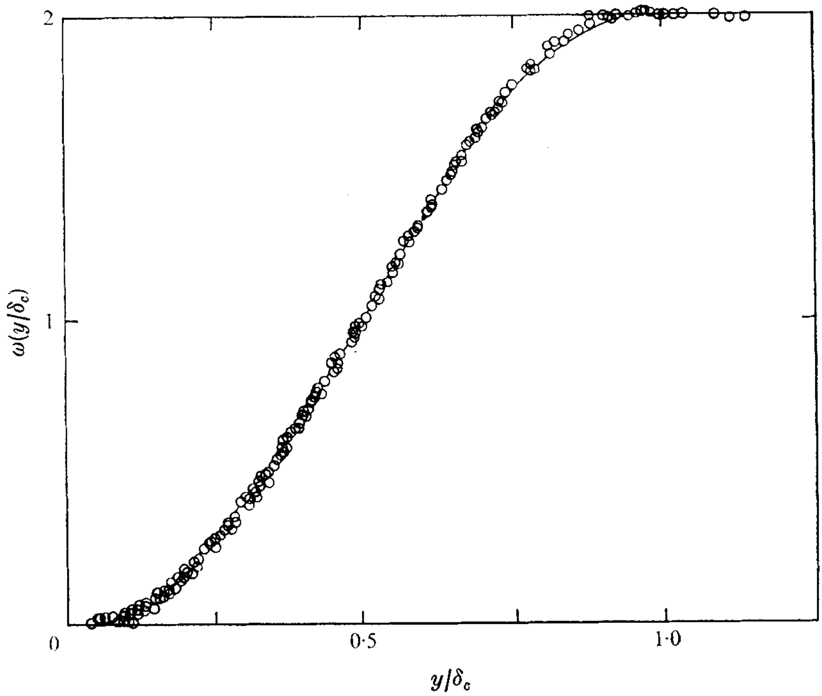

FIGURE 8. Wake components of the relaxing profiles. ——, equation (11).

small wake components except in the immediate vicinity of the perturbation. By contrast the boundary layers of series A and B have large well-defined wake components throughout.

Wake functions deduced from profiles in the reference layers (R and S) show excellent agreement with the Coles' wake function

$$\omega(y/\delta_c) = 2\sin^2(\tfrac{1}{2}\pi y/\delta_c), \tag{11}$$

as do most data for adverse-pressure-gradient layers (Coles 1968). Somewhat surprisingly, wake components of profiles after a step (series A and B) show almost the same excellent agreement (figure 8), which demonstrates once again the wide applicability of this empirical relationship. From the limited information available, it is difficult to explain the different behaviour of these data from those considered by Coles. A significant factor may be that the length scales associated with the wall perturbations in these tests were a considerably smaller fraction of the layer height than those for the data analysed by Coles.†

The variation of the wake strength factor for series A and B is compared with the reference-layer distributions in figure 9. Immediately after the step, Π has a value which corresponds closely to that for flow over a uniformly smooth wall at the same station. Further downstream of the step, the values of Π diverge

† Similar comments would apply to the Antonia & Luxton flows. However a valid comparison of their wake components is impossible owing to the failure of the universal law of the wall in the inner flow.

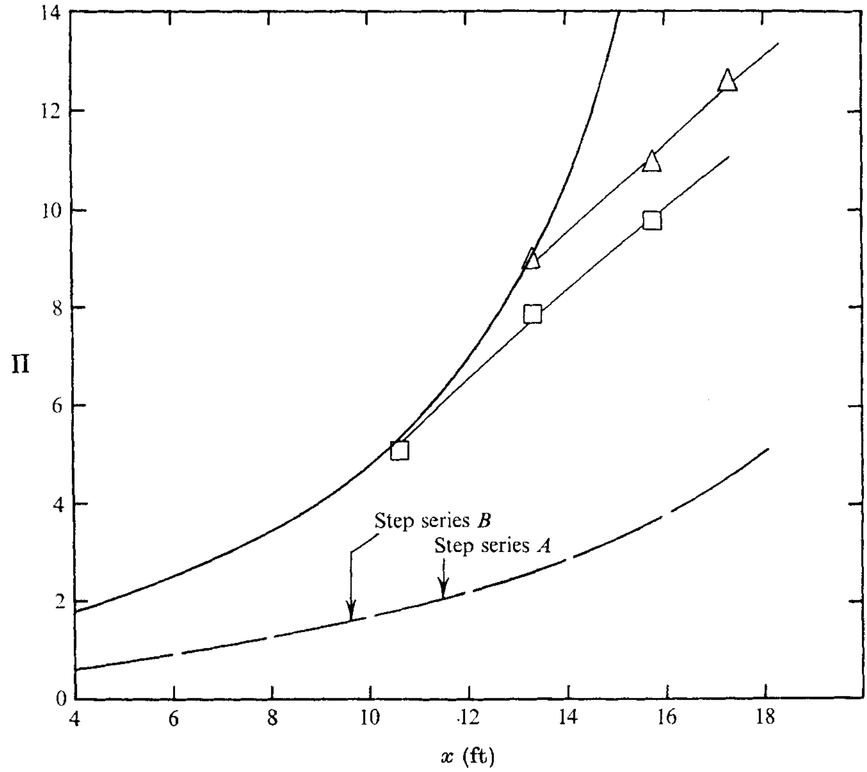

FIGURE 9. Π *vs.* x. ——, reference layer S; — —, reference layer R; △, series A; □, series B.

from the distribution for a uniformly smooth wall in a manner consistent with the similarity of outer profiles between layers and the wall shear-stress distributions.

Equilibrium considerations. In an undisturbed zero-pressure-gradient layer at high Reynolds number the Clauser profile parameter

$$G = \int_0^\delta \left(\frac{U_1 - u}{u_\tau}\right)^2 dy \Big/ \int_0^\delta \left(\frac{U_1 - u}{u_\tau}\right) dy$$

is constant and the flow is self-preserving. Perturbations applied to a zero-pressure-gradient layer cause G to vary from this constant value with a slow asymptotic return to equilibrium as the layer relaxes.

For layers with non-zero pressure gradients the relationship between G and β $(= \delta^* \tau_0^{-1} dp/dx)$ for all possible self-preserving layers has been the subject of theoretical treatments by Townsend (1961) and Mellor & Gibson (1966). An empirical relation representing a synthesis of theory and experimental results has been given by Nash (1965):

$$G(\beta) = 6{\cdot}1(\beta + 1{\cdot}81)^{\frac{1}{2}} - 1{\cdot}7. \tag{12}$$

If the locus of (G, β) for a boundary layer in an arbitrary adverse pressure gradient coincides with (12) then the layer passes through a series of self-

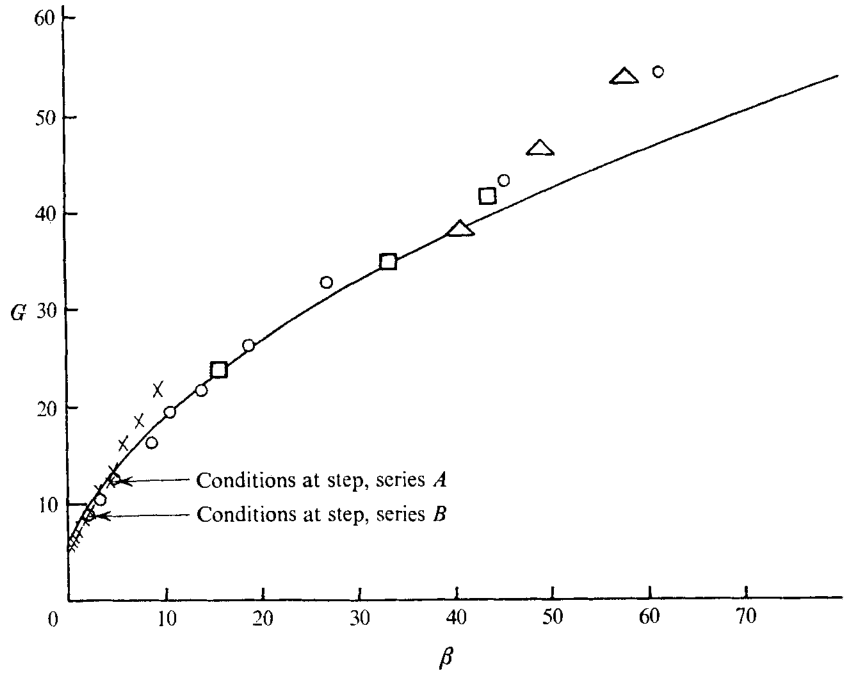

FIGURE 10. G *vs.* β. ×, rough-wall reference layer; ○, smooth-wall reference layer; △, series A; □, series B; ——, equation (12).

preserving states during its development. This type of flow could be termed 'locally self-preserving'. Experimental results analysed by Nash suggest that for layers in which $d\beta/dx > 0$ departures from (12) are small, and this is supported by Bradshaw's (1969) results. Conversely, results for layers in which $d\beta/dx < 0$ diverge rapidly from (12). Rotta (1962) analysed some unpublished measurements by Tillmann for which $d\beta/dx$ was first positive and then negative. He concluded that after a maximum in β the local value of G depended on the history of β.

The variation of G and β for the four present layers is shown in figure 10. Results for the two reference layers (in which $d\beta/dx > 0$†) deviate little from (12) and the layers are therefore (approximately) 'locally self-preserving'. Results for the two perturbed layers show a similar behaviour and presumably these layers are also locally self-preserving. Now in the present flows the severity M ($= \log z_1/z_2$) of the step change in roughness had values similar to those in the Antonia & Luxton (1972) flow (see figure 5) but whereas results for Antonia & Luxton's zero-pressure-gradient flow deviated substantially from self-preservation after the step the only effect on the present flows was a rapid increase in G (and β). The obvious interpretation of this evidence is that wall perturbations of a severity sufficient to destroy self-preservation in zero-pressure-gradient flow, when applied to adverse-pressure-gradient layers, do not destroy their

† Except between the last two profiles of the rough-wall reference layer (R11 and R12), where $d\beta/dx$ is slightly less than zero.

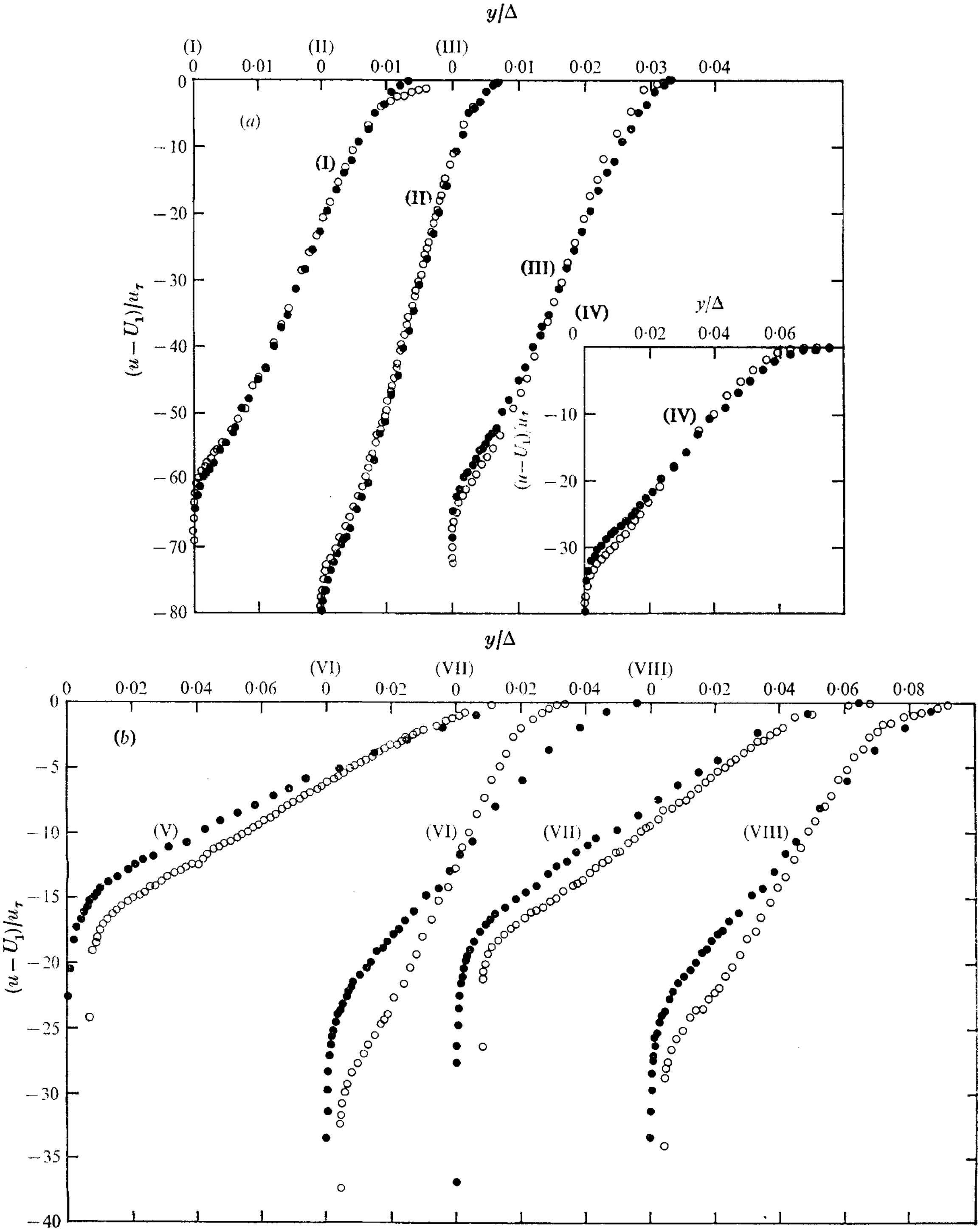

FIGURE 11. Comparison of velocity-defect profile shapes for profiles with similar local values of β. Profile data and symbols as in table 2. Data points have been left out of some profiles for clarity. Δ is Clauser's (1954) integral boundary-layer thickness:

$$\int_0^\delta \left(\frac{U_1-u}{u_\tau}\right) dy.$$

locally self-preserving development. Or alternatively wall perturbations have little effect on locally self-preserving development of adverse-pressure-gradient layers. However it could be that this particular experiment does not isolate the effect of wall perturbations on local self-preservation. The use of a rough-to-smooth step in an adverse-pressure-gradient flow dictated that $d\beta/dx$ (and M) remained positive across the step and as this is the empirical criterion for locally self-preserving flow deduced by Nash, it is perhaps not surprising that the layers showed only small deviations from (12). To separate the effects of pressure gradient and wall perturbations a useful experiment would be consideration of the case of a smooth-to-rough step in an adverse-pressure-gradient layer, where $d\beta/dx$ would be sharply negative after the step.

Velocity-defect shape. Clauser's proposal of one-parameter families of mean velocity profiles runs into difficulties in layers where pressure-gradient forces dominate throughout. The limiting case of such layers is the self-preserving layer generated by Stratford (1959), in which the wall shear stress was approximately zero throughout. This problem and related questions on the role of pressure gradient in deciding the profile shape for flows with large β has been the subject of proposals by Mellor & Gibson (1966) and McQuaid (1966).

Comparisons among the present set of four layers approaching separation in the same pressure gradient but with different wall shear histories offer some insight into the relative importance of pressure gradient and wall shear in determining defect profile shape. Pairs of profiles from different layers but with closely similar values of β were selected for comparison. The data were found to contain eight pairs of profiles for which the difference in β between the two profiles was less than 10%. Table 2 lists values of flow parameters for these profiles. The eight pairs of profiles have been divided into two groups.

In the first group, the profiles of each pair have the same shape when plotted in defect co-ordinates (figure 11*a*). The agreement between the two profiles deteriorates slightly but progressively from pair I to pair IV and this is matched by a slight but progressive disparity in β agreement between the profiles of the pairs. An interesting feature of this group is the relative upstream variations of β and wall shear. In all four cases the profiles of each pair had grossly different histories of these two parameters. Apparently β history and wall shear history has had little influence in determining the defect shape of these profiles.

In the second group of profiles, values of β are matched in each pair, with a precision similar to that for the first group. The difference in β values for each pair increases slightly from pair V to pair VIII. In this case however, the profiles of each pair are markedly different when plotted in defect co-ordinates (figure 11*b*). A significant difference evident between the two groups is that in the first group the local values of the pressure gradient dp/dx and the pressure-gradient history are similar, whereas in the second group they are not. If we accept Rotta's (1962) assertion that the local magnitude of the wall shear has little influence on a profile's velocity-defect shape, then the evidence suggests that similar defect profile shapes are produced in layers at similar local values of β, provided that both the history and local values of the pressure gradient are similar. It may be that only one of these conditions (in addition to β similarity)

Profile number (see figure 1) and symbols used in figure 11			Local values: β	Local values: G	Local values: dp/dx (p.s.f./ft)	Local values: $c_f' \times 10^3$	Parameter history: β	Parameter history: c_f'	Parameter history: dp/dx
First group									
I	*B*3	○	43·5	41·89	0·255	0·34	Very different	Very different	Similar
	*S*9	●	45·4	43·18	0·244	0·32			
II	*A*3	○	57·5	53·72	0·193	0·24	Very different	Very different	Similar
	*S*10	●	61·2	54·48	0·197	0·23			
III	*A*2	○	49·0	46·43	0·255	0·30	Very different	Very different	Similar
	*S*9	●	45·4	43·18	0·244	0·32			
IV	*B*1	○	15·7	23·91	0·633	0·72	Different	Very different	Similar
	*S*6	●	14·0	21·58	0·455	0·80			
Second group									
V	*S*2	●	3·30	10·53	1·78	1·77	Similar	Very different	Very different
	*R*7	○	3·20	11·33	0·633	3·45			
VI	*S*4	●	8·85	16·32	0·908	1·12	Similar	Very different	Very different
	*R*11	○	9·25	21·88	0·255	1·55			
VII	*S*3	●	4·77	12·65	1·19	1·47	Very similar	Very different	Very different
	*R*9	○	4·48	12·23	0·40	3·00			
VIII	*S*4	●	8·85	16·32	0·908	1·12	Different	Different	Very different
	*R*12	○	7·18	18·41	0·193	1·80			

TABLE 2. Summary of profile parameters

is necessary but further evidence is required to resolve the matter. Evidence presented by Rotta (1962) of different profile shapes generated at the same local value of β but with different β histories is not necessarily in disagreement with the present proposal. However as pressure-gradient details for the data were not published this cannot be tested.

4. Conclusion

(i) In the present experimental investigation of turbulent boundary layers approaching separation in a strong adverse pressure gradient, it is not surprising to find that pressure-gradient forces modify the response of the layer to a wall perturbation. What is perhaps instructive is a consideration of those features of the response which are unaffected by the application of an adverse pressure gradient to the flow. The central feature of flow over a step change in roughness is the generation of a new internal layer downstream of the step. The height of this new internal layer appears to depend on the nature of the new conditions at the wall as it scales with the local roughness length of that wall.

In non-dimensional terms the internal-layer height is approximately proportional to distance from the step.

Universal logarithmic distributions of mean velocity were established downstream of the step in spite of the severe discontinuity in surface conditions and strong pressure gradients. Establishment of wall similarity after the step appears to have been very rapid. At a distance of two layer thicknesses downstream of the step the extent of wall similarity normal to the wall was comparable with that in a corresponding unperturbed layer.

The wall shear stress implied by the logarithmic distributions showed an unusually orderly adjustment to the new wall conditions. Immediately downstream of the step the wall shear attained the equilibrium value with little or none of the overshooting displayed by similar flows on flat plates or in ducts. Downstream of the step the wall shear slowly diverged from the distribution for a corresponding flow on a uniform smooth wall.

In zero-pressure-gradient flow it has been observed that the outer layer reacts very slowly to changes in wall conditions. It is therefore not surprising to find in adverse-pressure-gradient flow that the outer layer, which is dominated by pressure-gradient forces, responds even more slowly to a change in wall conditions. So slow is this response that mean velocity profiles of the perturbed layer are very similar to corresponding profiles from a reference layer on a uniformly rough wall. The unusual structure obtained by matching this 'rough wall' outer layer to a wall layer of greatly reduced shear can still accurately be described by the Coles wall–wake combination.

(ii) The variation of Clauser's profile parameter G in adverse-pressure-gradient layers over a step does not appear to give the simple description of the departure and return to equilibrium conditions that it gives in zero-pressure-gradient layers. Variation of G with β for the present layers would suggest that they continue to develop with local self-preservation throughout the initial relaxation process after the step. It is probably more accurate to conclude that the single profile parameter G cannot distinguish between a layer developing in local self-preservation and a layer relaxing after a severe wall perturbation in which $d\beta/dx$ remains positive. A layer in which G remains constant during development (a Clauser equilibrium layer) is probably the only pressure-gradient case in which a perturbation will cause a variation in G which can be related with certainty to the departure from, and return to, self-preserving flow.

(iii) The limited experimental data suggest that profiles having identical defect shapes are produced in adverse-pressure-gradient layers at positions where the values of Clauser's parameter β are similar, provided that the pressure-gradient history and local values of the pressure gradient are also similar. It is possible that only one of these additional restraints is necessary. However the data were inadequate to separate the effects of the two parameters.

The measurements for this paper were taken in the University of Melbourne's wind tunnel. The author wishes to thank Professor P. N. Joubert and Dr. A. E. Perry for their assistance.

REFERENCES

Antonia, R. A. & Luxton, R. E. 1971*a* *J. Fluid Mech.* **48**, 721.

Antonia, R. A. & Luxton, R. E. 1971*b* *Trans. A.S.M.E., J. Basic Engng*, **93**, 22.

Antonia, R. A. & Luxton, R. E. 1971*c* *Phys. Fluids*, **14**, 1027.

Antonia, R. A. & Luxton, R. E. 1972 *J. Fluid Mech.* **53**, 737.

Bradshaw, P. 1969 *Aero. Res. Counc. R. & M.* no. 3575.

Bradshaw, P. & Ferriss, D. H. 1965 *Nat. Phys. Lab. Aero. Rep.* no. 1145.

Bradshaw, P. & Wong, F. Y. F. 1972 *J. Fluid Mech.* **52**, 113.

Clauser, F. H. 1954 *J. Aero. Sci.* **21**, 91.

Clauser, F. H. 1956 *Adv. in Appl. Mech.* **4**, 21.

Coles, D. E. 1953 Ph.D. thesis, California Inst. Tech.

Coles, D. E. 1956 *J. Fluid Mech.* **1**, 191.

Coles, D. E. 1968 *AFOSR–IFP Stanford Conf. on Comp. Turbulent Boundary Layers*, vol. 2, p. 1.

Klebanoff, P. S. & Diehl, Z. W. 1951 *N.A.C.A. Tech. Note*, no. 2475.

McQuaid, J. 1966 *Aero. Res. Counc. Current Paper*, no. 885.

Makita, H. 1968 M.Eng. thesis, University of Tokyo (see Tani 1968).

Mellor, G. L. & Gibson, D. M. 1966 *J. Fluid Mech.* **24**, 255.

Moore, W. L. 1951 Ph.D. thesis, State University of Iowa.

Nash, J. F. 1965 *Agardograph*, no. 97, p. 253.

Perry, A. E. 1966 *J. Fluid Mech.* **26**, 481.

Perry, A. E. & Joubert, P. N. 1963 *J. Fluid Mech.* **17**, 193.

Perry, A. E., Schofield, W. H. & Joubert, P. N. 1969 *J. Fluid Mech.* **37**, 383.

Rotta, J. C. 1962 *Prog. Aero. Sci.* **2**, 134.

Schofield, W. H. 1969 Ph.D. thesis, University of Melbourne.

Stratford, B. S. 1959 *J. Fluid Mech.* **5**, 17.

Tani, I. 1968 *AFOSR–IFP Stanford Conf. on Comp. Turbulent Boundary Layers*, vol. 1, p. 483.

Taylor, R. J. 1962 *J. Fluid Mech.* **13**, 529.

Tillmann, W. 1945 *U. & M.* no. 6627 (Trans. 1946 *Ministry Aircraft Production, Rep. & Trans.* VG34-T).

Townsend, A. A. 1961 *J. Fluid Mech.* **11**, 97.

Townsend, A. A. 1965 *J. Fluid Mech.* **22**, 773, 799.

Wood, D. H. & Antonia, R. A. 1974 *C. Kolling Res. Lab., University of Sydney, Rep.* T.N.F.-68.